Int. J. Electrochem. Sci., 4 **(2009)** 377 - 385

International Journal of ELECTROCHEMICAL SCIENCE
www.electrochemsci.org

Influence of $CeCl_3$ and Deposition Parameters on Electroless NiFeP Deposition

Wei-Qing Huang[1,*], *Jian-Qin Deng*[1], *Guo-Fang Huang*[2]

[1] College of Physics and Microelectronics Science, Hunan University, Changsha 410082, China
[2] Changsha Nanfang Vocational College, Changsha 410208,China
[*]E-mail: weiqinghuang@hnu.cn

Received: 5 December 2008 / *Accepted:* 30 January 2009 / *Published:* 1 March 2009

The NiFeP deposits were prepared by electroless deposition. The influences of the rare earth element, temperature and bath pH on the deposition rate, mixed potential, deposit composition and structure were systematicly discussed. The results reveal that the deposition rate decreases with the addition of rare earth due to the competition adsorptions between rare earth cerium cations, iron ions, nickel ions, and/or hypophosphite, and the formation of new catalytic center resulting from hyalrcxide colloid. The increase of bath temperature and pH will lead to an increase of deposition rate. The deposition rate deduced from polarization experiments show similar trend with that determined by gravimetrical measurements. The content of phosphorus in the deposit decreases first with the addition of $CeCl_3$ in bath, then increases with further addition of $CeCl_3$. XRD analysis indicates that the adding of cerium increases the crystalline of the deposit.

Keywords: electroless plating, FeNiP, rare earth, deposition rate, composition, structure

1. INTRODUCTION

Iron group-rare earth deposits exhibit low Curie temperatures and strong temperature dependence of coercivity, making them ideal candidates with read, write, and erase capabilities for high density storage media[1-4]. Numerous Iron group- rare earth alloy deposits have been prepared by various vacuum deposition processes[5-8]. Chemical deposition is a simple technology to prepare homogeneous films on various substrates[9-12]. It has numerous advantages over physical deposition technologies, such as, less costly and easily maintained equipment, requiring less energy and space, and relatively low temperature operating conditions. Moreover, deposits composition, structure and their properties can be tailored by varying bath composition and operating conditions.

Rare earth metals are extremely base metals with reduction potentials being negative to -2 V, indicating that their deposition may not be readily obtained owing to the onset of vigorous hydrogen evolution. Recently, iron group alloys with rare earth elements have been electrodeposited from aqueous solutions, which was explained as induced codeposition[13-14]. Electroless deposition is a chemical method to obtain homogeneous films on various substrates and is applied in wide industrial fields. Researches have been demonstrated that doping with RE elements can improve the performances of electroless deposits[15]. In this paper, $CeCl_3$ was added into NiFeP electroless bath. The influence of Ce addition, as well as the bath temperature and pH, on the deposition rate, composition, and structure of deposits is investigated.

2. EXPERIMENTAL PART

A basic hypophosphite reduced electroless sulphate bath was chosen as the plating bath, and the chemical compositions of electroless NiFeP plating bath are listed in table 1. The pH of the solution was adjusted using NH3.H2O to 10 and the bath temperature was controlled at about 70°C except if stated otherwise. Copper was used as substrate with size of 25×15×2 mm for gravimetrical measurements. As copper is not a catalytic substrate for chemical deposition from hypophosphite solutions, the NiFeP deposition was initiated galvanically using aluminum at the beginning of the electroless process[10,16-17]. The mass of deposits was calculated by weighing the samples before and after deposition by electronic microbalance model HT-300. The average deposition rate was determined by dividing the deposit mass by the surface area of substrate and deposition time.

Table 1. Chemical compositions of electroless Ni-Fe-P plating bath

Reagent	Concentration, g/L
$(NH_4)_3C_6H_5O_7$	40
$(Na)_3C_6H_5O_7{\cdot}2H_2O$	48.5
$FeSO_4{\cdot}7H_2O$	15
$NiSO_4{\cdot}6H_2O$	7.5
$NaH_2PO_2{\cdot}H_2O$	33
$C_{12}H_{12}O_{11}$	2
CeCl3	0-0.9
$NH_3{\cdot}H_2O$	25 mL/L

Polarization experiments were carried out in a three-compartment cell with the electrochemical analyzer CHI-660B. A platinum foil with size 20mm×40mm was used as an auxiliary electrode and a saturated calomel electrode were used as reference electrode. The working electrode was the copper electrode (φ = 19 mm) embedded in an epoxy resin. In order to simulate partial cathodic or anodic reactions, the investigation of the electrolytes in the absence of either the reductant $Na_2H_2PO_2$ (oxidation solution) or the metal salts $FeSO_4$ and $NiSO_4$ (reducing solution) was carried out. The

polarization curves were obtained by scanning the potential in the range ±150 mV of the mixed potential E_{mix}, and the scanning rate was 1 mV s^{-1}.

The deposits' compositions were examined using scanning electron microscopy (SEM, JEOL JSM—6700) combined with energy dispersive spectrometry (EDS). The structure of the deposit was analyzed by XRD (Siemens D5000).

3. RESULTS AND DISCUSSION

Fig.1 shows that the deposition rate decreases with the increasing of $CeCl_3$. This can be easily understood. With peculiar electronic structure and unique behavior, rare earth cerium will adsorb preferentially at the surface on the substrate. The adsorbed cerium tends to give away electrons and part cerium becomes cations due to the low electronegativity, which change the interface structure of electrode, hinder the diffusion and deposition of the metal ions, thus lead to the decrease of deposition rate. In addition, cerium cations may form hyalrcxide colloid in alkaline solutions with excessive $CeCl_3$ addition, which acts as the catalytic center causing the intense self-catalyzed reaction in the bath solution, thus further lower the effective deposition rate.

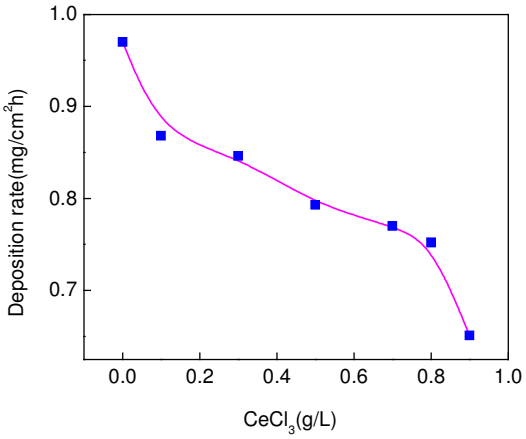

Figure 1. The dependency of the deposition rate on the concentration of $CeCl_3 \cdot 7H_2O$

The temperature of electroless bath is one of the important factors affecting the deposition rate. Fig.2 depicts the dependence of the deposition rate on the temperature. At low temperatures, the process is very slow. When the temperature varies from 50 to 70°C, the deposition rate increases with increasing temperature linearly, however, the deposition rate decreases slightly with the further increase of temperature. As is known, the temperature increasing facilitates the ion diffusion and decreases the energy barrier for cathodic and anodic reaction, leading to the increase of the deposition rate. The slight decrease of deposition rate beyond 70 °C maybe attributed to the drastic movement of ions and the formation of selfcatalytic activity center in the bath, resulting the decrease of the virtual deposition rate on the substrate. The dependence of the deposition rate on the pH is presented in Fig. 3.

It can be clearly seen that the pH has the most significant influence on the deposition rate of the electroless process, which increases with the pH increasing. The deposition rate changes by more than a factor of 10 when the pH varies from 8.5 to 10.5.

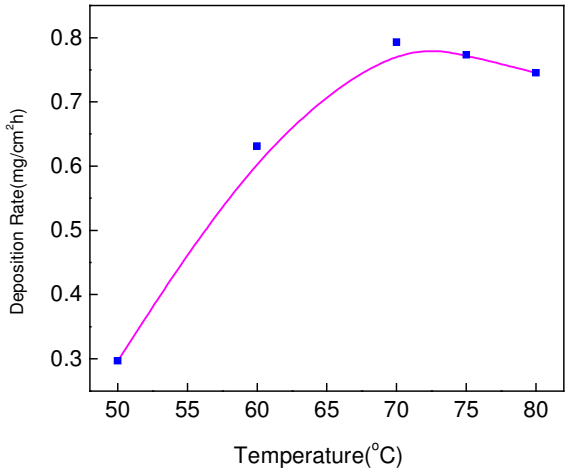

Figure 2. Effect of bath temperature on the deposition rate

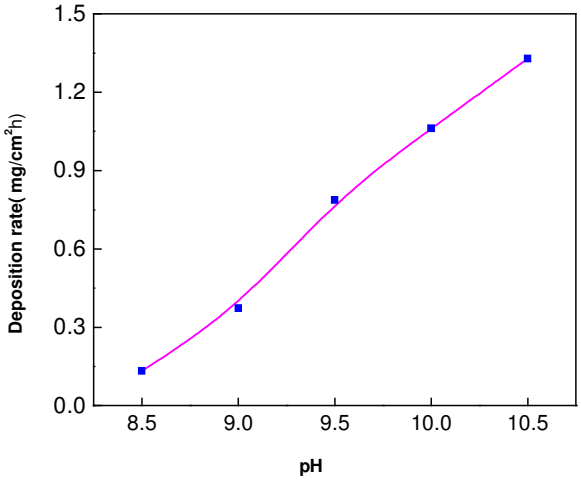

Figure 3. Effect of bath pH on the deposition rate

It has widely been accepted that electroless deposition proceeds along the electrochemical mechanism as a simultaneous reaction of cathodic metal deposition and anodic oxidation of a reductant at the same catalytic surface. The difference between the redox potential of the reducing agent and that of the metal, ΔE, is the force to drive deposition. The *I–E* curves in oxidation solution and reducing solution are displayed in Fig. 4. The redox potential in reducing solution is -1.02 V vs.SCE, and those in oxidation solution with different $CeCl_3$ concentration are shown in Fig.5. As shown in Fig.5, the redox potential in oxidation solution is positive to that in reducing solution, the potential difference ΔE

is larger than zero, which is the force to drive deposition. The redox potential of metal salt shifts negatively, i.e. the potential difference ΔE decreases with the increase of $CeCl_3$ concentration. In addition, the polarization resistance of the cathodic curve near the redox potential can be calculated, which increases with the addition of cerium ions in the bath, suggesting that the cerium ions inhibit the cathodic reduction process. It can also be seen from Fig. 4 that the cathodic and anodic curves intersect at one point. According to the Wagner–Traud mixed potential theory, the coordinates of intersection of anodic and cathodical polarization curves represent the deposition current density and the mixed potential, which are displayed in Fig.5. Fig.5 clearly shows that the mixed potential shifts cathodically and the deposition current density decreases with the $CeCl_3$ increasing, which accords with the gravimetrical measurements. The deposition current changes by more than a factor of 2 when the $CeCl_3$ concentration increaes from 0 to 0.9g/L. The decrease of deposition rate can be attributed to the decrease of deposition force and the increase of the cathodic polarization resistance with the addition of $CeCl_3$ in the bath.

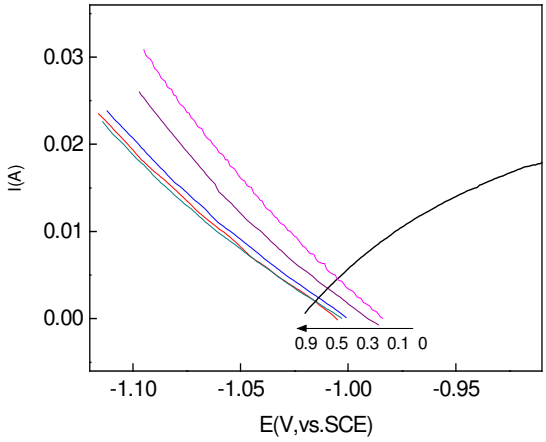

Figure 4. *I–E* curves for oxidation of hypophosphite and for reduction of metal ions with different $CeCl_3 \cdot 7H_2O$ concentration

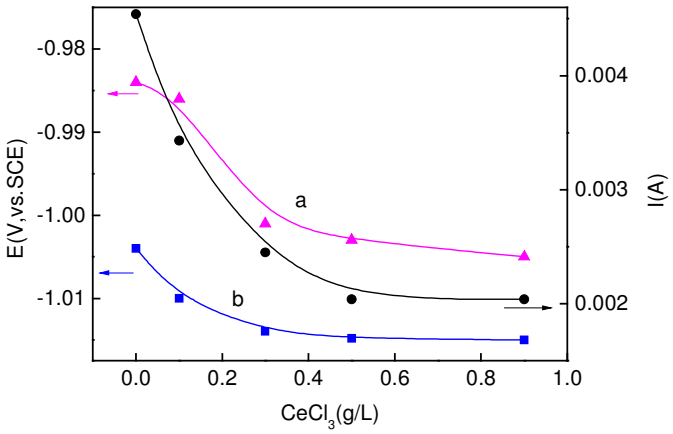

Figure 5. Dependence of the mixed potential and current density on the $CeCl_3 \cdot 7H_2O$ concentration a. The redox potential with different $CeCl_3 \cdot 7H_2O$ concentration in oxidation solution b. The mixed potential according to the coordinates of intersection of anodic and cathodical polarization curves

Fig. 6 depicts the dependence of the mixed potential and deposition current on the temperature, as derived from electrochemical measurements. When the temperature varies from 50 to 75℃, the mixed potential changes little and the deposition current increases linearly with increasing temperature.

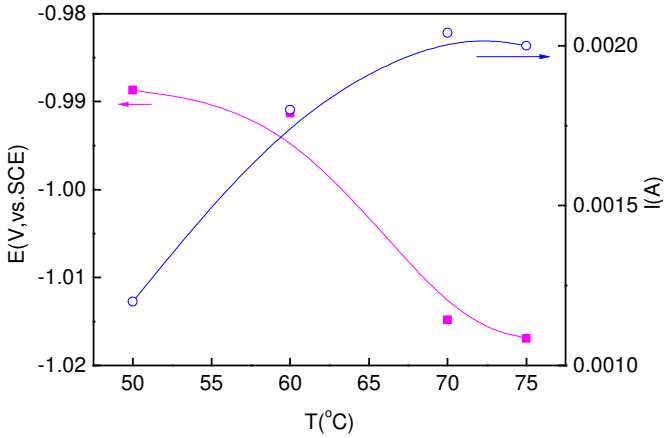

Figure 6. Dependence of the mixed potential and current density on the bath temperature

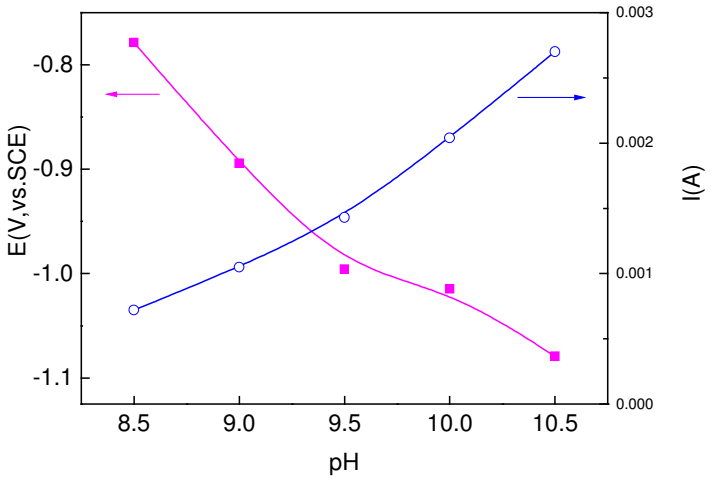

Figure 7. Dependence of the mixed potential and current density on the bath pH

The dependence of the mixed potential and deposition current density on the pH, as derived from the polarization curves, is presented in Fig. 7. It can be seen that the mixed potential shifts cathodically and the deposition current density increases with the pH increasing. The mixed potential shifts by approximately 300mV and the deposition current density changes by more than a factor of 3 when the pH varies from 8.5 to 10.5. This trend was also observed for electroless Co–W–P and Co–P deposition [18]. As discussed above, deposition parameters have great effect on the deposition rate, it is useful to optimize the deposit by choosing the reasonable parameter. Moreover, the deposition rate

deduced from polarization experiments show similar trend with that determined by gravimetrical measurements, indicating the electroless NiFeP deposition obeys the mixed potential theory.

Table 2. The dependence of Fe-Ni-P deposits compositions on $CeCl_3 \cdot 7H_2O$ concentration

$CeCl_3 \cdot 7H_2O$ Concentration, g/L	P	Fe	Ni
0	26.12	4.38	69.50
0.1	22.59	4.26	73.15
0.5	25.64	3.88	70.48

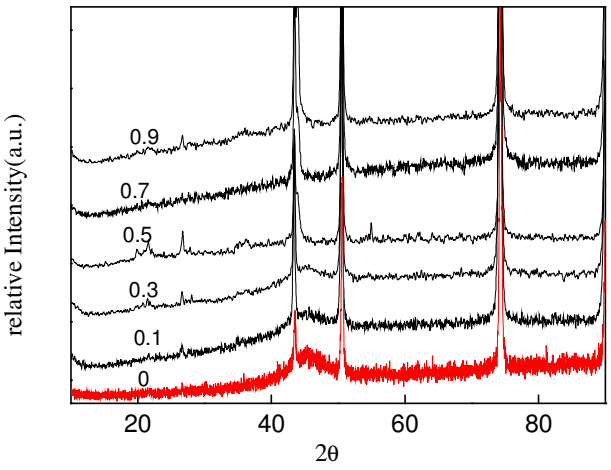

Figure 8. The XRD patterns of deposits prepared with different $CeCl_3 \cdot 7H_2O$ concentration

We now turn to investigate the effect of cerium on the composition and structure of NiFeP deposits. Table 2 shows the deposit composition as a function of the concentration of $CeCl_3$. By adding 0.1g/L $CeCl_3$ into the bath, the content of phosphorus and iron in the deposit decreases, while that of nickel increases. However, as the concentration of $CeCl_3$ increases to 0.5 g/L, the content of phosphorus in the deposit increases slightly, while that of nickel and iron decreases. The change of phosphorus content in the deposit can be attributed to the peculiar electronic structure and the unique behavior of rare earth Ce. Theoretically, the electronegativity of rare earth Ce is very low (about -2eV), so it is hard to initiate the deposition of alloys with cerium from aqueous solution. The cerium atoms can be adsorbed on the substrate surfaces preferentially during the deposition. Due to the low electronegativity of Ce, part element Ce give away electrons and part cerium becomes cations. It is known that electroless deposition results from the anodic reactions (oxidations of reducing agent) and cathodic reactions (reduction of the metallic species, reducing agent and protons), both are occurred on

the same catalytic surface. In the case of NiFeP electroless deposition, the electrons released due to the oxidation of $H_2PO_2^-$ are obtained competitively by Fe^{2+}, Ni^{2+}, H^+ and/or $H_2PO_2^-$ to reduce, thus lead to the formation of NiFeP deposits. The positively charged cerium cations may form neutral molecule with $H_2PO_2^-$, thus hinders the reduction of hypophosphite and lead to the decrease of phosphorus content in the deposit. However, excessive cerium adsorption will change the electronic shell structure of electrode interface, which baffles the diffusion and reduction of iron and nickel ions, leading to an increase of phosphorus in the deposit. The structure of NiFeP deposits can be changed by the addition of the $CeCl_3$ in the bath. The XRD patterns of NiFeP deposits are displayed in Fig.8. It can be seen clearly that there is a diffused peak near 42^o as the $CeCl_3$ concentration lower than 0.3 g/L, however, there appear a sharp peak as the $CeCl_3$ concentration beyond 0.5 g/L. The half-widths of peaks decreases with the concentration of $CeCl_3$, indicating the increase of the deposit crystalline.

Table 3 shows the deposit composition as a function of the bath temperature. As the temperature increase from 60 to 80 ºC, the content of phosphorus and nickel in the deposit increases, while that of iron decreases, suggesting that temperature increasing facilitates the competitive reduction of nickel and $H_2PO_2^-$ ions.

Table 3. The dependence of Fe-Ni-P deposits compositions on the bath temperature

T(ºC)	P	Fe	Ni
60	25.44	4.27	70.29
70	25.64	3.88	70.48
80	25.85	3.47	70.68

4. CONCLUSIONS

The effects of $CeCl_3 \cdot 7H_2O$ on the deposition rate, composition and structure of electroless NiFeP deposit were analyzed. It is shown that the deposition rate decreases with the increasing of $CeCl_3 \cdot 7H_2O$ due to the competition adsorptions between rare earth cerium and metal ions, hypophosphite on the surface of the substrate, which change the interface and the ion diffusion, decrease the deposition force and increase the cathodic polarization resistance. The phosphorus content in the deposit decreases first, then increases with the addition of $CeCl_3 \cdot 7H_2O$, which can be attributed to the peculiar electronic structure and the unique behavior of rare earth cerium. The deposition parameters, such as bath pH and temperature, also have great effect on the deposition rate and the deposit composition. It is useful to optimize the deposit by choosing the reasonable parameters.

References

1. M. Getzlaff, R. Pascal, R. Wiesendanger, *Surf. Sci*., 566-568 (2004) 236

2. L. A. Stone, H. V. Snelling, A. G. Jenner, *Appl. Surf. Sci*., 109-110 (1997) 389
3. V. Oderno, C. Dufour, K. Dumesnil, Ph. Mangin, G. Marchal, *J. Cryst. Growth*, 165 (1996) 175
4. M. Matsuura, R. Petkie, G. Singco, K.N. Tu, *Mater. Sci. . Eng*. A, 133 (1991) 551
5. Z. H. Hu , X. H. Cheng , M. G. Zhu , W. Li, F. Z. Lian, *Rare Metals*, 27 (2008) 358
6. X. W. Li, C. Song, J. Yang, F. Zeng, K. W. Geng, F. Pan, *J. Magn. Magn. Mater*. 315 (2007) 120
7. F. Yildiz, S. Kazan, B. Aktas, S. I. Tarapov, L. Tagirov, B. Granovsky, *J. Magn. Magn. Mater*. 305 (2006) 24
8. V. Madurga, C. Favieres, J. Vergara, *J. Non-Cryst. Solids* 353 (2007) 941
9. A. Kohn, M. Eizenberg, Y. Shacham-Diamand, *J. Appl. Phys*., 94 (2003) 3810
10. G. F. Huang, W. Q. Huang, L. L. Wang, Y. Meng, Z. Xie, B. S. Zou, *Electrochim. Acta*, 51 (2006) 4471
11. A. Vaskelis, J. Jaciauskiene, I. Stalnionien, E. Norkus, *J. Electroanal. Chem*. 600 (2007) 6
12. G. F. Huang, J. Q. Deng, W. Q. Huang, L. L. Wang, B. S. Zou, L. Dong*, Int. J. Electrochem. Sci*., 2 (2007)72
13. S. Deki, K. Kuratani , M. Uemura, K. Akamatsu, M. Mizuhata, A. Kajinami, *Thin Solid Films* 460 (2004) 83
14. M. Schwartz, N. V. Myung, K. Nobe, *J. Electrochem. Soc*. 151 (2004) C468
15. Y. Meng, L. L. Wang, G.F. Huang, W. Q. Huang, B. S. Zou*, Int.J.Mat.Res*. 98 (2007) 217
16. W. Q. Huang, G. F. Huang, L. L. Wang, X. G. Shi, *Int. J. Electrochem. Sci*., 3 (2008) 1316
17. G. F. Huang, W. Q. Huang, L. L. Wang, B. S. Zou, Q. L. Wang, J. H. Zhang, *Int. J. Electrochem. Sci*., 3 (2008) 145
18. N. Petrov, Y. Sverdlov, Y. Shacham-Diamand*, J. Electrochem. Soc*. 149 (2002) C187